Wireless Link SNR Mapping Onto An Indoor Testbed*

Jing Lei, Roy Yates, Larry Greenstein, Hang Liu

WINLAB
Rutgers University
73 Brett Road, Piscataway, NJ 08854, USA
{michelle, ryates, ljg, hliu}@winlab.rutgers.edu

Abstract

To facilitate a broad range of experimental research on novel protocols and application concepts, we employ an indoor wireless testbed to emulate the performance of the real-world networks. A fundamental issue for emulation is the replication of communication links of specified quality. In particular, we need to replicate on the testbed, for every link in the real world, a communication link whose received signal-to-interference-and-noise-ratio (SINR) matches the corresponding link signal-to-noise-ratio (SNR). In this paper, we focus on the downlink SNR mapping associated with a network with a single access point (AP). Four indoor wireless propagation models (commercial buildings with/without line of sight path and residential buildings with/without line of sight path) and two types of geometric distributions (uniform distribution inside a circular cell and uniform distribution along a line) have been investigated. Based on the characteristics of the indoor testbed, we propose a mapping method with one AP and one interferer, which separates the task into two phases: in the first phase, the best location and transmission power for the interferer node are determined; in the second phase, the topology of receiver nodes is configured by a minimum weight matching algorithm. Through analysis and simulations, we find that when the interferer node is located on the corner across from the AP, we can achieve the mapping range on the order of 57dB and average mapping error on the order of 2dB.

Keywords

Indoor Testbed, Path Loss, Downlink, SNR, Minimum Weight Matching

1. INTRODUCTION

The powerful technology and market trends towards portable computing and communications imply an increasingly important role for wireless access in the next-generation Internet. New sensor and pervasive computing applications are expected to drive large-scale deployments of embedded computing devices interconnected via new types of short-range wireless networks. Motivated by the goal to advance the technology innovation in the wireless networking field, the Open Access Research Testbed for Next-Generation Wireless Networks (ORBIT) project focuses on the creation of a large-scale wireless network testbed which will facilitate a broad range of experimental research on novel protocols and application concepts [1]. The proposed ORBIT system employs a two-tier laboratory emulator/field trial network to achieve reproducibility of experimentation, and supports evaluation of protocols and applications in real-world settings illustrated in Fig. 1 (a). As shown by Fig.1 (b), the laboratory-based wireless network emulator is constructed with a large two-dimensional array of 802.11x radio nodes (~400 nodes), which are uniformly spaced on a grid of 20 meters by 20 meters and can be dynamically interconnected into specified topologies for reproducible wireless channel models.

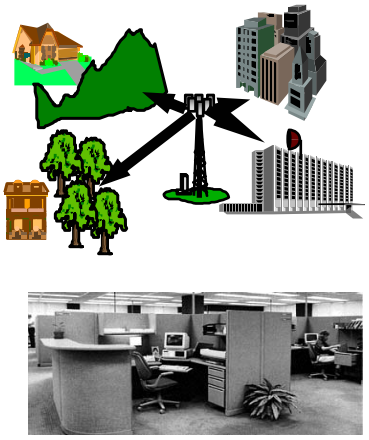

(a) Real world outdoor/indoor environment

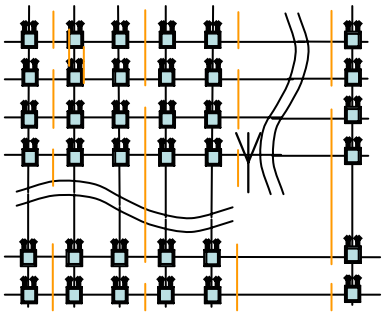

(b) ORBIT testbed with 400 nodes uniformly distributed on a grid of 20m by 20m

Fig.1 Mapping of real world environments onto the ORBIT indoor testbed

This research is supported by NSF ORBIT Testbed Project (NRT Grant # ANI0335244.)

A fundamental issue for emulation is the replication of communication links of specified quality. In particular, we need to map the actual link signal-to-noise-ratio (SNR) onto the indoor testbed. The difficulties of this task lie in the facts that on the grid, due to the limited path loss gains, we can only obtain a link SNR range of approximately 26 dB. In addition, the path loss between the grid nodes can only take on discrete values. Consequently, we dedicate one or more nodes on the grid to the radiation of noise interference, which has the effect of increasing the dynamic range of received signal-to-interference-and-noise-ratio (SINR) values among the other grid nodes. This permits the set of grid SINRs obtained by our mapping method to better match the set of real-world link SNRs.

In this paper, our discussion focuses on the downlink SNR mapping for a real-world network with a single access point (AP) and multiple wireless terminals. In order to avoid a time consuming, brute-force search over the entire grid, we have proposed a two-phase mapping method based on the minimum weight matching [2] between the real-world link SNRs and the grid SINRs. As for the mapping of uplink SNRs, it can be easily realized by adjusting the transmission power of each mapped grid node within the 20+ dB dynamic range.

The rest of this paper is organized as follows: Section 2 introduces the link SNR model for real-world indoor WLAN applications; Section 3 formulates the proposed mapping algorithm; finally, Section 4 presents the simulation results and concludes this paper.

2. Link SNR OF INDOOR WLAN

2.1 Pathloss Model

In a wireless network, the propagation environment can vary from a simple line-of-sight (LOS) path to one that is attenuated by various obstructions [3]. To obtain the link SNR samples for indoor environments, we extend the path loss models developed for ultra-wide-band (UWB) communications [4] to WLAN applications. Similar to [4,5], we separate the indoor path loss models into commercial (COM) and residential (RES) buildings, as well as line-of-sight (LOS) and non-line-of-sight (NLS) paths. To capture the differences in building materials, structures and ages, we assume both the path loss exponent and the shadowing term as random variables, which are given by

$$\alpha = \mu_\alpha + x_\alpha \sigma_\alpha \tag{1}$$

and

$$s = y(\mu_s + x_s \sigma_s) \quad , \tag{2}$$

respectively, where $\mu_\alpha, \sigma_\alpha, \mu_s$ and σ_s are building-dependent constants, while x_α, x_s and y are mutually independent Gaussian random variables of zero mean and unit variance. The values for x_α and x_s vary from building to building, but y varies from location to location inside each building. Table 1 lists the model parameters for four different indoor environments. Substituting (1) and (2) into the generic path loss formula [3] yields

$$PL(d) = \underbrace{PL_0 + 10\mu_\alpha \log_{10}(d/d_0)}_{\text{average path loss}} + \underbrace{10x_\alpha\sigma_\alpha \log_{10}(d/d_0) + y\mu_s + yx_s\sigma_s}_{\text{deviation from the average value}} \underbrace{\qquad}_{\text{shadowing}} . \tag{3}$$

Table 1. Parameters for link SNR models

Propagation Models	PL_0 (dB) d_0=1 m	Pathloss Exponent		Shadowing	
		μ_α	σ_α	μ_s	σ_s
LOS Commercial	43.7	2.04	0.3	1.2	0.6
NLS Commerical	47.3	2.94	0.61	2.4	1.3
LOS Residential	47.2	1.82	0.39	1.5	0.6
NLS Residential	50.4	3.34	0.73	2.6	1.9

Considering the limitations of practical environments, it is more realistic to model the distribution of x_α, x_s and y as truncated Gaussian variates. Therefore, we introduce the following truncations:

$$|x_\alpha| \le 1.3 \quad , \tag{4.1}$$

$$|x_s| \le 1.5 \quad , \tag{4.2}$$

$$|y| \le 1.5 \quad . \tag{4.3}$$

The constraint (4.1) yields a truncated path loss exponent falling within the 10th to 90th percentiles of the Gaussian distribution, while (4.2) and (4.3) lead to truncated distributions for the mean and deviation of the shadowing that fall within the 7th to 93th percentiles.

2.2 Noise and Interference

Given the transmission power and path loss models, it is the received noise and interference that determines the minimum acceptable received power. Generally, natural background noise and devices' internal noise can be minimized by good system design. Beyond this, levels of artificial noise/interference may set the sensitivity limit of a receiver. Sources of artificial noise/interference include other communication systems operating in the same frequency band, or operating in other frequency bands but unintentionally generating RF signals in the band of interest. For example, microwave ovens operate at a natural frequency of the water molecule of approximately 2.45 GHz, which falls in the middle of Wi-Fi band. Also, the oscillators used in some microwave ovens have poor stability and have been observed to vary by 10MHz around their nominal frequencies. In addition, due to the limited frequency spectrum resource, communication frequencies are reused the world over, leading to multiple access interference. As a result,

the formula for calculating the ratio of signal-to-interference-and-noise (SINR) is

$$SINR = \frac{P_S \beta_S}{\eta + \sum_{k=1}^{\Gamma} P_{I_k} \beta_{I_k}} \quad (5)$$

where η is the noise power, P_S and P_{I_k} denote the transmission power of the desired user and the *k*-th interferer, respectively, Γ is the number of interferers, and β_S and β_{I_k} represent the path loss of receiver *k* to the desired user and the interferer *k*, respectively.

Following [3], the noise power can be calculated via

$$\eta = N_0 W \ , \quad (6)$$

where *W* is the equivalent noise bandwidth and N_0 is the power spectral density of thermal noise, which can be expressed by

$$N_0 = kT_0F \ , \quad (7)$$

where *k* is the Boltzmann constant, *F* is the noise figure and T_0 is the absolute temperature. In our link SNR model, the contribution of interference is ignored due to the interference suppression mechanism of the MAC layer, and we take *F=10* dB and $T_0 = 290\ K$.

2.3 Geometric Distribution of Receivers

In a wireless network, the receive terminals can be distributed in quite different ways. In the following, we will consider the probability density function associated with two forms of geometric distribution.

- receivers are uniformly distributed inside a circular cell, with the AP at the center:

$$f_D(d) = \frac{2d}{R^2 - r^2} \ , \ r \le d \le R \ ; \quad (8)$$

- receivers are uniformly distributed along a line, with the AP at one end:

$$f_D(d) = \frac{1}{R - r} \ , \ r \le d \le R \ ; \quad (9)$$

where *r* denotes the reference distance of the path loss model, *R* represents the coverage radius of the AP, and *d* is the random distance of T-R separation.

3. Link SNR Mapping by Grid SINR

In this section, our discussion is focused on the case of downlink SNR mapping for a WLAN with a single AP. As an abstract of Fig.1 (b), Fig.2 (a) shows a total of 400 nodes uniformly spaced inside a square. To map the link SNR onto the grid channel, we can classify the nodes into three categories: access points (AP), interferers and receive terminals. Basically, the freedom of grid nodes that can be exploited for SNR mapping includes the following:

- Transmission power of AP
- Number, locations and transmission powers of interferers
- Topology of AP, interferers and receive terminals

Obviously, we only have a finite number of grid nodes and their path losses can only take on discrete values. Therefore, for a given setting of the AP transmission power, we cannot find a perfect match for arbitrary link SNRs and have to develop mapping techniques to minimize the difference between the target SNRs and the mapped grid SINRs.

In order to avoid a time consuming, brute-force search over the entire grid of nodes, we have developed a mapping method based on the minimum weight matching algorithm. Assume the square grid has N^2=400 uniformly distributed nodes, and there are *M* link SNRs required to be mapped onto the grid. The basic idea of our approach can be formulated as follows:

- Pick one node as the access point (AP) and fix it to a grid corner.
- Choose another node as the interferer and position it along a diagonal of the grid (with the AP at one end of this diagonal);
- From the remaining 398 grid nodes, select a subset of M nodes as the receive terminals. Configure the topology of these receiver nodes to make the vector of grid SINRs best match the vector of link SNRs in the mean square sense.

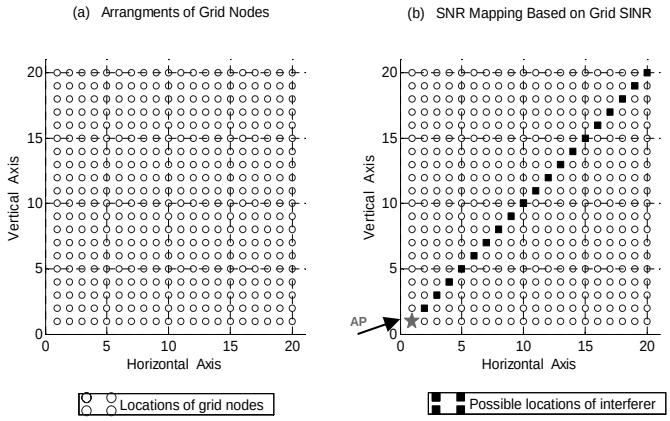

Fig. 2 Illustration of proposed mapping methodology

Fig.2 (b) illustrates the proposed mapping methodology. The pentagon on the corner represents the AP whose position is fixed, and the filled squares on the diagonal stand for the possible locations of the interferer. For simplicity, we can choose one diagonal node as the interferer and leave the remaining 400-2=398 nodes as candidates for the M receive terminals. Roughly, the mapping task can be separated into two phases:

- Coarse Mapping: choosing the location of the interferer node and configure its transmission power;
- Fine Mapping: determining the locations of the receivers.

In the first phase, we can figure out a best position and power level for the interferer. In the second phase, we do the "fine mapping" by invoking the minimum weight assignment algorithm to determine the topology of the receivers.

Substituting $\Gamma = 1$ into (5) and assuming $\eta << \beta_I(k)P_I$, where P_I denotes the transmission power of the interferer, and $\beta_I(k)$ stands for the path loss between receiver k ($1 \le k \le 398$) and the interferer, the SINR of node k can be simplified into

$$SINR(k) \approx \frac{P_S}{P_I} \cdot \frac{\beta_S(k)}{\beta_I(k)} = SIR \cdot \frac{\beta_S(k)}{\beta_I(k)} \ , \qquad (10)$$

where $SIR = P_S / P_I$ is the transmission power ratio between the AP and the interferer. The second term on the right hand side of (10) is the ratio of path losses. Once the position of AP is fixed, this ratio depends on the distance between the interferer and the receiver only. Furthermore, for a specified SIR, the SINR distribution is asymptotically determined by the position of the interferer only. In other words, if the histogram of the grid SINR is plotted as a function of the SIR parameterized on the interferer, we can observe that the pattern of the histogram is determined by the position of the interferer while the relative translation of the histogram for a given interferer is dependent on the SIR. Without loss of generality, Fig.3 (a)-(b) present the cumulative distribution function (CDF) of the grid SINR for interferer nodes 5 and 19, respectively, with SIR (transmission power of AP vs. transmission of interferer) as a parameter. It can be seen from these figures that the shape of the CDF curves corresponding to the same interferer are identical, and the translation among these curves depends on the SIR.

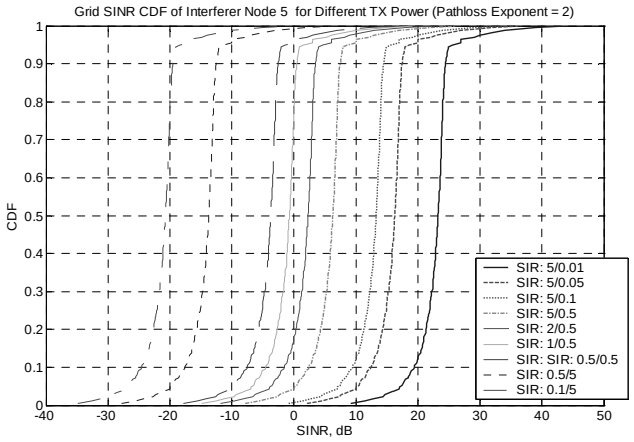

(a) Node 5

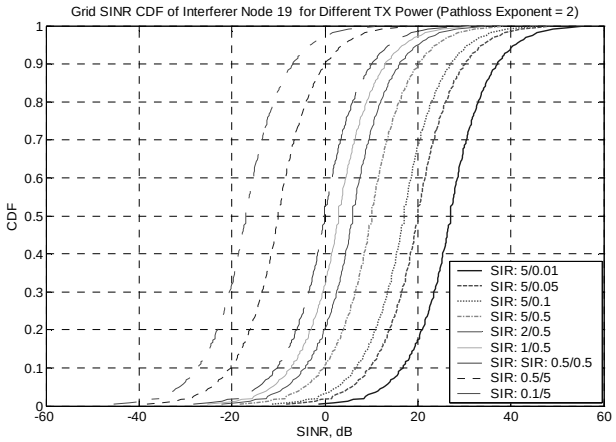

(b) Node 19

Fig.3 CDF of grid SINR for interferer nodes 5 and 19 with different transmission power settings

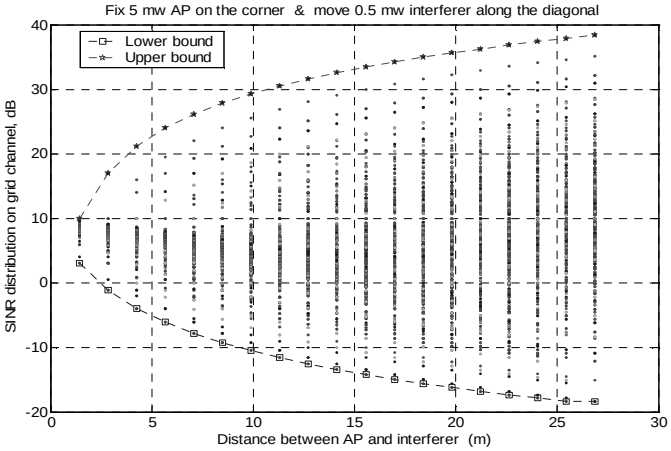

Fig. 4 Distribution of grid SINR for different locations of the interferer

Fig.4 shows the distribution of the grid SINRs corresponding to different locations of the dedicated interferer when we fix the 5mw AP on one corner, and move the dedicated interference source along the diagonal of the grid. From this figure, we can see that the mapping range is determined by the location of the interferer. The farther away the interferer from the AP, the larger the mapping range. Since the largest mapping range is approximately 57 dB, which is sufficient for most applications of our interest, we can simplify the configuration of interference source by fixing the interference source to node 19, which is located on the farthermost corner across the AP. As a result, the task of coarse mapping reduces to the power setting for node 19 only.

Finally, the steps for coarse mapping can be generalized as follows:

- Fix the position of the unique AP to a grid corner.
- Fix the position of the unique interferer to the grid corner across the AP.
- Compute the median of the target link SNR samples.
- Make the SIR of the grid channel equal to the median calculated above and set the transmission power of the interferer node in line with the SIR.

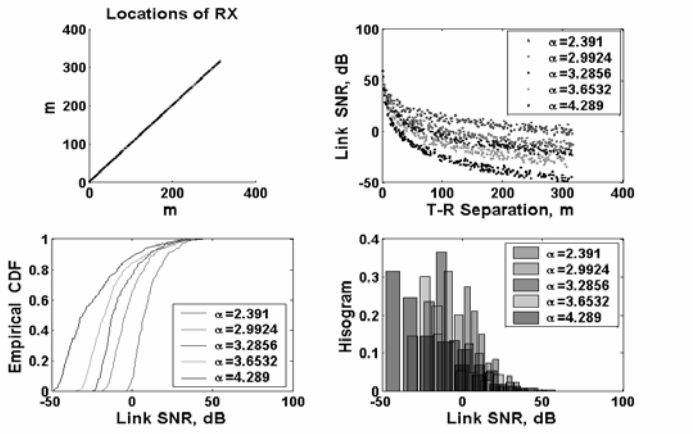

Fig. 5 Simulated link SNR for NLS/RES environments (RX along a line)

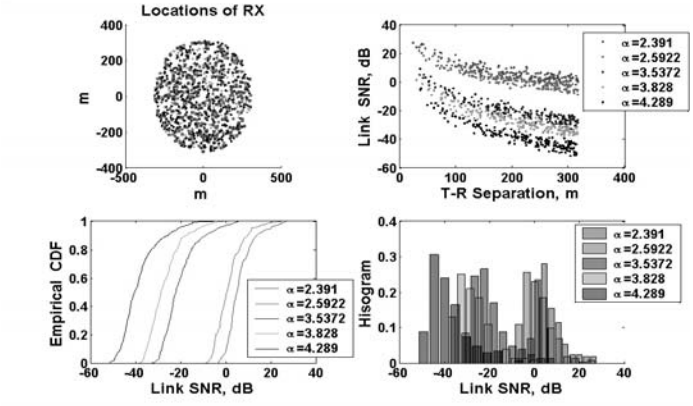

Fig. 6 Simulated link SNR for NLS/RES environments (RX inside a circle)

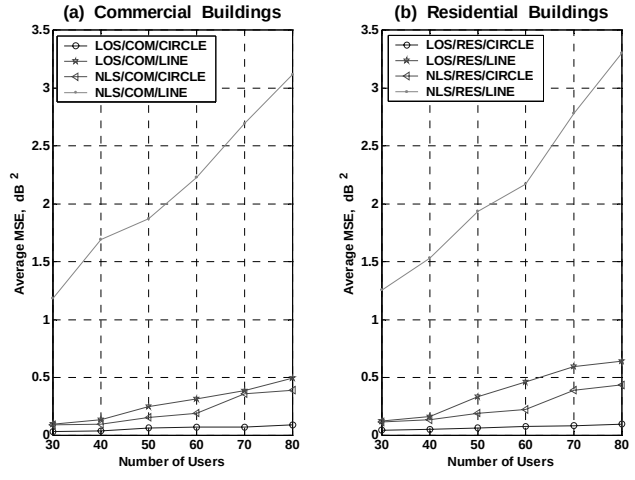

Fig. 7 Average MSE vs. number of users under different scenarios
(a) inside commercial buildings
(b) inside residential buildings

After the transmission power of the interferer is determined, the fine mapping can be implemented by invoking a bipartite weighted matching algorithm. In our case, we regard the M target link SNRs and the K grid SINRs as two sets of vertices, whose dB values are given by sets $\{\gamma_m\}_{m=1}^{M}$ and $\{\rho_k\}_{k=1}^{K}$, respectively. For each element in set $\{\gamma_m\}_{m=1}^{M}$, we need to assign it to a distinct element in $\{\rho_k\}_{k=1}^{K}$, and the rule governing the assignment is given by:

$$\text{Minimizing} \quad \sum_{m,k} \mu_{m,k} \left(\gamma_m - \rho_k\right)^2$$

$$\text{subject to} \sum_{k=1}^{K} \mu_{m,k} = 1, \forall\, m \in \{1,2\cdots M\} \qquad (11)$$

$$\text{where } \mu_{m,k} = \begin{cases} 1, & \gamma_m \text{ is assigned to } \rho_k \\ 0, & \text{otherwise} \end{cases}$$

4. Results

Without loss of generality, Fig. 5 and Fig. 6 show the distribution of link SNR under NLS/RES environments when the receive terminals are uniformly distributed inside a circle and along a line, respectively. The SNR samples are generated by the statistical models given by (3) and (4.1)-(4.3). The receive terminals are assumed to be uniformly distributed inside an arc and along a line, respectively. Obviously, even under the assumptions of the same propagation and geometric distribution, there is significant difference in the range and distribution of link SNR due to the randomness of path loss exponent and shadowing.

Fig.7 shows the average mapping MSE (defined as the mean of squared difference between the actual link SNR and the matching value given by the grid SINR) versus the number of link SNR samples under four indoor environments (LOS COM, NLS COM, LOS RES, NLS RES) and two geometrical distributions (RX along a line, RX inside an arc). Under each scenario, we consider *M*, the number of real-world nodes whose SNRs are to be mapped onto the grid, to be 30, 40, 50, 60, 70 and 80. It can be observed from this figure that NLS environments have larger mapping error than LOS environments because the path loss exponents for the LOS case comes closer to that of free space propagation (we assume free space propagation on the grid channel). Besides, the "RX inside a circle" distribution can achieve better mapping accuracy than "RX along a line" distribution because in the latter case it is more probable to get large SNR values which are beyond the coverage of the grid SINR. Therefore, of the eight scenarios considered, the NLS/COM/Line and NLS/RES/Line cases have average MSE significantly larger than the remaining cases. The performance discrepancy between them and the remaining cases is caused mainly by the difference of path loss exponents, as indicated by Fig. 5 and Fig. 6. Because of the larger path loss in NLS scenarios, the dynamic range of link SNRs is more probable to exceed the coverage of

the grid. In our experiments, we have observed link SNR ranges over 80 dB, and the mapping MSE is dominated by the outliers (links with extremely small or large SNR) which are not of our research interest. Moreover, the mapping MSE can be reduced by trimming the SNRs of the outliers to appropriate levels.

5. Conclusions

Based on the characteristics of the ORBIT indoor testbed, we have proposed a link SNR mapping method with one AP and one interferer. Through analysis and simulations, we have found that when the interferer node is located on the corner across from the AP, we can achieve the mapping range on the order of 57dB and average mapping error on the order of 2dB.

Our future work includes the link SNR mapping for ad hoc network, which is more complicated than the AP case due to the multiple constraints imposed on the grid nodes. To simplify the mapping task, we shall consider the quantized SNR levels.

References

[1] D. Raychaudhuri, "ORBIT: Open-Access Research Testbed for Next-Generation Wireless Networks", proposal submitted to NSF Network Research Testbeds Program, May 2003.

[2] C. H. Papadimitriou and K. Steiglitz, Combinatorial Optimization: Algorithms and Complexity, Prentice Hall, 1982.

[3] T. S. Rappaport, Wireless Communications: Principles and Practice, Prentice Hall, 1995.

[4] S. S. Ghassemzadeh, L. J. Greenstein, A. Kavcic, T. Sveinsson and V. Tarokh, "UWB indoor path loss model for residential and commercial buildings", Proc. of. VTC 2003-Fall, Volume 5, pp. 3115 – 3119.

[5] V. Erceg, L. J. Greenstein, S. Y. Tjandra, S. R. Parkoff, A. Gupta, B. Kulic, A.A. Julius, R. Bianchi, "An empirically based path loss model for wireless channels in suburban environments" , IEEE Journal on Selected Areas in Communications, Volume 17, pp. 1205 – 1211, July 1999.